



ECE335 Introduction to Electronic Devices

**Project 2**  
**Design of a Deep Submicron NMOS**

December 6, 2023

Liza Babaoglu 1006026532	
Deniz Uzun 1006035005	

The Edward S. Rogers Sr. Department of Electrical & Computer Engineering  
University of Toronto

## Introduction

This report examines the simulations of deep submicron NMOS transistors in the Sentaurus TCAD tool in our project. We investigate the relationship between various doping concentrations and their subsequent impact on the device's behavior. For example, we will design an NMOS by testing and selecting appropriate halo and source/drain extension doping concentrations to mitigate short-channel effects inherent to these small devices, 45nm gate length NMOS transistors. Our goal is to refine the design to satisfy specific  $I_{off}$  and  $I_{on}$  thresholds for two different applied voltages ( $V_{dd}$ ), and observe plots in linear and saturation regimes. We will also define some key terms, discuss the effect on transistors, and compare the device's parameters against benchmarks from TSMC's paper on 65nm CMOS.

## Methodology

### A. Background Reading and Getting Started

The initial section of the report defines key concepts like extension doping, halo doping, and spacer. We then plot the 2D doping concentration of the NMOS transistor in Sentaurus with default values. We also integrated insights from the TSMC paper into our background research.

### B. Design

We used the Sentaurus 2022 version. We first designed our NMOS transistor to desired  $I_{off} \leq 35 \text{ nA}/\mu\text{m}$  and  $I_{on} \geq 700 \text{ }\mu\text{A}/\mu\text{m}$  for  $V_{dd} = 1\text{V}$  by changing the substrate doping concentration, dopant concentration of the extension region, and dopant concentration of the halo region. Based on the effects of these concentrations on the threshold voltage and currents, we tested various numbers in a systematic method. We plotted the linear and saturation regime currents plots using the visualization tools. Then, we designed another NMOS transistor to desired  $I_{off} \leq 0.01 \text{ nA}/\mu\text{m}$  and  $I_{on} \geq 445 \text{ }\mu\text{A}/\mu\text{m}$  for  $V_{dd} = 1.2\text{V}$  by similarly changing the substrate doping concentration, dopant concentration of the extension region, and dopant concentration of the halo region.

## Results and Discussion

### A. Background Reading and Getting Started

1. *Extension doping* is created to slightly reduce channel length by extending the source and drain toward each other using low-energy dopant implants of the same dopant type as the source and drain [1]. It results in smaller channel length, increased threshold voltage, and reduced short-channel effects [1] [2].

*Halo doping* is done by placing the dopants just below the active channel, adjacent to the source and drain regions, in order to avoid the punch-through between the source and drain through the bulk substrate in short-channel devices [3]. The halo limits the downward, and more importantly, the lateral diffusion of the source and drain. The second advantage is that depletion width is reduced without compromising the channel threshold voltage. [1]

*Spacers*, also called sidewalls, insulate the drain and source metal contacts from the gate of the transistor [4]. Spacers provide a large electric field without allowing large current leakage and reduce the effect of interface traps on carrier population [4]. They enable lateral displacement of heavily doped source/drain regions from the edges of the transistor gate, which is beneficial in reducing short channel effects of submicrons and deep submicron transistors [5].

2.

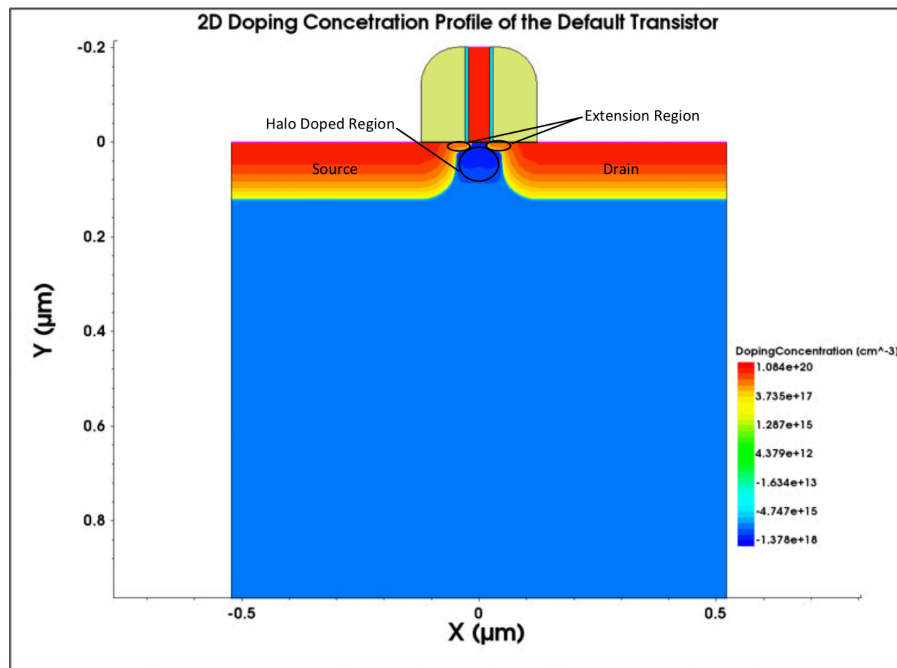


Figure 1: 2D doping concentration profile of the default N-MOSFET

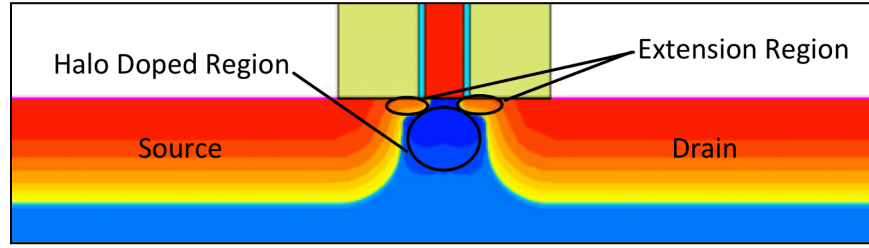


Figure 2: Magnified image of the region near the channel for the default N-MOSFET

3. From the TSMC paper [6] and electronics glossary [7]

- |                      |                                |                                |
|----------------------|--------------------------------|--------------------------------|
| i) LP: Low Power     | ii) G: General Purpose         | iii) HS: High Speed            |
| iv) IO: Input/Output | v) HVT: High Threshold Voltage | vi) LVT: Low Voltage Threshold |

4. Higher  $I_{on}$  and lower  $I_{off}$  in MOS are desirable. A higher  $I_{on}$ , which is the current when the transistor is on, implies that the transistor can deliver more current to the load, which is beneficial for performance as it allows for faster switching and higher drive capabilities. This is especially important in circuits where the transistors' speed directly affects the processing unit's overall speed. As seen in Table 1 of the TSMC paper [6], HS applications have larger  $I_{on}$  values (ex: NMOS  $I_{on}$  in HS STD is  $1010 \mu A/\mu m$  vs. G STD is  $795 \mu A/\mu m$  vs. in LP STD is  $570 \mu A/\mu m$ ). Whereas lower  $I_{off}$ , the current when the transistor is off, contributes to lower power consumption when the device is in standby mode, especially for high-density integrated circuits to minimize power dissipation and manage thermal issues. As seen in Table 1 of the TSMC paper [6], LP applications have lower  $I_{off}$  values (e.g. NMOS  $I_{on}$  in LP STD is  $0.2 nA/\mu m$  vs. G STD is  $26 nA/\mu m$  vs. in HS STD is  $80 nA/\mu m$ ).

## B. Design

### 1. Final Design

The  $I_{on}$  and  $I_{off}$  values of our final design is  $I_{on} = 728.7 \mu A/\mu m$  and  $I_{off} = 29.67 nA/\mu m$ . To achieve these results the substrate doping (SubDop) was set to  $9 \times 10^{17} cm^{-3}$ , halo doping (HaloDop) was set to  $3.3 \times 10^{18} cm^{-3}$  and extension doping (ExtDop) was set to  $6 \times 10^{19} cm^{-3}$ . The design specifications, including various geometric parameters and doping parameters are given in Table 1. Labeled 2D doping concentration profile of the designed transistor and its magnified view

near the channels are presented in *Figures 3 and 4*. The Sentaurus Workbench showing the achieved device specification is presented in *Figure 5* and summarized in Table 2.

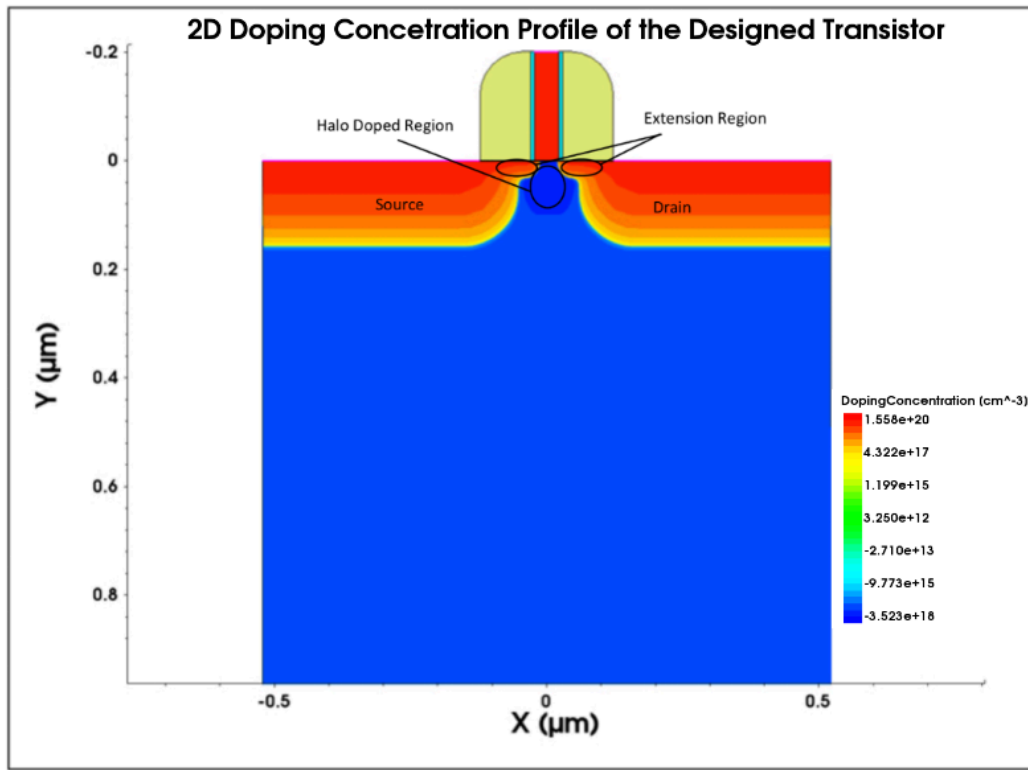


*Figure 3: 2D doping concentration profile of the designed N-MOSFET*

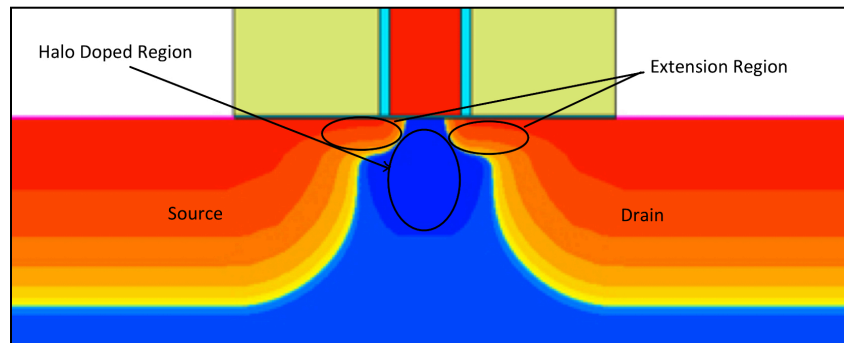


*Figure 4: Magnified image of the region near the channel of the designed N-MOSFET*

Vtgm	VtLin	IdLin	SSlin	gmLin	IdSat	Ioff	VtISat	SSsat	gmSat	Ron
0.440	0.382	9.857e-05	88.525	2.473e-04	7.287e-04	2.967e-09	0.262	87.305	1.320e-03	3488.387

*Figure 5: Screenshot of the Sentaurus Workbench, showing the achieved device specifications*

$$(I_{off} = 29.67 \text{ nA}/\mu\text{m} \leq 35 \text{ nA}/\mu\text{m} \text{ and } I_{on} = 728.7 \mu\text{A}/\mu\text{m} \geq 700 \mu\text{A}/\mu\text{m} \text{ for } V_{dd} = 1V)$$

Table 1: Summary of transistor parameters of our final design

Parameters (notation)	Value
Substrate doping concentration (SubDop)	$9.0 \times 10^{17} \text{ cm}^{-3}$
Dopant concentration of the extension region (ExtDop)	$6.0 \times 10^{19} \text{ cm}^{-3}$
Dopant concentration of the halo region (HaloDop)	$3.3 \times 10^{18} \text{ cm}^{-3}$
Depth of the extension region (XjExt)	$0.12 \text{ } \mu\text{m}$
Depth of the halo region (XjHalo)	$0.07 \text{ } \mu\text{m}$
Depth of the source and drain (XjSD)	$0.12 \text{ } \mu\text{m}$
Spacer Length (Lsp)	$0.1 \text{ } \mu\text{m}$
Gate Thickness (Hpol)	$0.2 \text{ } \mu\text{m}$
Oxide Thickness (Tox)	$1.4 \text{ nm}$

Table 2: Summary of transistor specifications from our final design [8]

Specifications (notation)	Value
Threshold voltage defined as the intersection of the tangent at the maximum $g_m$ with the $V_{gs}$ axis ( $V_{tgm}$ )	$0.440 \text{ V}$
Threshold voltage defined as $V_{gs}$ at which $I_d = 100 \text{ nA/L}_g$ for $V_{ds} = V_{dlin}$ ( $V_{tiLin}$ )	$0.382 \text{ V}$
$I_d$ at $V_{ds} = V_{dlin}$ and $V_{gs} = V_{dd}$ ( $I_{dLin}$ )	$9.857 \times 10^{-5} \text{ A}/\mu\text{m}$
Subthreshold voltage swing at $V_{ds} = V_{dlin}$ ( $SS_{lin}$ )	$88.525 \text{ mV/decade}$
Maximum transconductance at $V_{ds} = V_{dlin}$ ( $g_{mlin}$ )	$2.473 \times 10^{-4} \text{ S}/\mu\text{m}$
Saturation current $I_d$ at $V_{ds} = V_{gs} = V_{dd}$ ( $I_{dSat}$ )	$7.287 \times 10^{-4} \text{ A}/\mu\text{m}$
Off-state (drain-leakage) current $I_d$ at $V_{ds} = V_{dd}$ and $V_{gs} = 0 \text{ V}$ ( $I_{off}$ )	$2.967 \times 10^{-9} \text{ A}/\mu\text{m}$
Threshold voltage defined as $V_g$ at which $I_d = 100 \text{ nA/L}_g$ for $V_{ds} = V_{dd}$ ( $V_{tiSat}$ )	$0.262 \text{ V}$
Subthreshold voltage swing at $V_{ds} = V_{dd}$ ( $SS_{sat}$ )	$87.305 \text{ mV/decade}$
Maximum transconductance at $V_{ds} = V_{dd}$ ( $g_{mSat}$ )	$1.320 \times 10^{-3} \text{ S}/\mu\text{m}$
On-state output resistance ( $R_{on}$ )	$3488.387 \text{ } \Omega\mu\text{m}$

## 2. Design Process

In this section we will summarize the impactful changes we have conducted. We began our design process for the NMOS transistor with the default parameters listed in Table 1 with the default values of the substrate, halo, and extension regions.

```
(define SubDop 1e17 ); (define HaloDop 1.5e18 ); (define ExtDop 1e19) ; [1/cm3])
```

The respective transistor specification and their values are seen below:

Vtgm	VtiLin	IdLin	SSlin	gmLin	IdSat	Ioff	VtiSat	SSsat	gmSat	Ron
0.220	0.200	5.265e-05	80.637	1.605e-04	5.163e-04	1.828e-07	0.093	83.261	7.030e-04	4705.770

*Figure 6: Screenshot of the Sentaurus Workbench of the default transistor*

As seen from the specifications,  $I_{dsat}$  was lower than our desired values, and  $I_{off}$  was higher than desired values. Hence, increasing or lowering *both* currents simultaneously would not have fixed this issue, that is,  $I_{on}$  should increase while  $I_{off}$  should decrease. Therefore, in our first iteration we focused on increasing the substrate doping to increase the threshold voltage, thereby reducing  $I_{off}$ . Usually, increasing threshold voltage reduces  $I_{on}$ , however, during short channel effects, it is possible to see the beneficial increase in  $I_{on}$ , as seen from the specifications below. After several iterations and evaluations, we settled on a substrate doping of  $9 \times 10^{17} \text{ cm}^{-3}$ .

```
(define SubDop 9e17 ); (define HaloDop 1.5e18 ); (define ExtDop 1e19) ; [1/cm3])
```

Vtgm	VtiLin	IdLin	SSlin	gmLin	IdSat	Ioff	VtiSat	SSsat	gmSat	Ron
0.246	0.212	6.850e-05	84.772	1.866e-04	6.157e-04	1.358e-07	0.108	85.889	6.531e-04	4582.454

*Figure 7: Screenshot of the Sentaurus Workbench of the 1st iteration*

In our second iteration, our focus was on increasing  $I_{on}$ . We raised  $I_{on}$  by enhancing the extension doping, because increasing the extension doping enhances the electrical conductivity in the source/drain extensions, thereby reducing the series resistance and allowing more current to flow, which increases  $I_{on}$ . This indeed increased  $I_{off}$  as well, but we will fix that in our next iteration.

```
(define SubDop 9e17 ); (define HaloDop 1.5e18 ); (define ExtDop 6e19) ; [1/cm3])
```

Vtgm	VtiLin	IdLin	SSlin	gmLin	IdSat	Ioff	VtiSat	SSsat	gmSat	Ron
0.236	0.170	1.227e-04	96.169	2.708e-04	1.107e-03	1.917e-06	0.007	111.039	1.455e-03	2025.854

*Figure 8: Screenshot of the Sentaurus Workbench of the 2nd iteration*

In our third iteration, our focus was on decreasing  $I_{off}$ . By increasing the doping concentration of the halo region, we raised the threshold voltage in the lateral direction under the gate edges, which helped to reduce  $I_{off}$ . Since this was our last parameter to change, we used a systematic tabular format to test different values for halo doping, reaching the desired current values at a halo doping of  $3.3 \times 10^{18} \text{ cm}^{-3}$ .

```
(define SubDop 9e17); (define HaloDop 3.3e18); (define ExtDop 6e19) ; [1/cm3])
```

Vtgm	VtiLin	IdLin	SSlin	gmLin	IdSat	Ioff	VtiSat	SSsat	gmSat	Ron
0.440	0.382	9.857e-05	88.525	2.473e-04	7.287e-04	2.967e-09	0.262	87.305	1.320e-03	3488.387

*Figure 9: Screenshot of the Sentaurus Workbench of the 3rd and final working iteration*

### 3. Final Design Plots for $I_d$ vs. $V_{gs}$

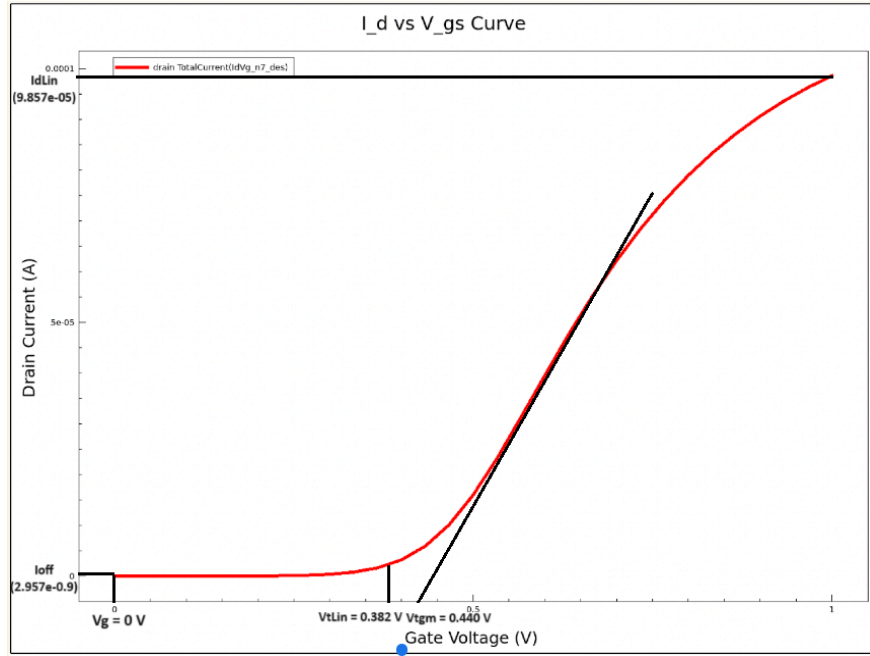


Figure 10:  $I_d$  vs.  $V_{gs}$  curve where  $0 < V_{gs} < V_{dd}$  for  $V_{ds} = 50$  mV (Linear region)  
 $V_{tLin} = 0.382$  V,  $I_{off} = 2.967 \times 10^{-9}$  A and  $I_{dLin} = 9.857 \times 10^{-5}$  A is marked on the plot.

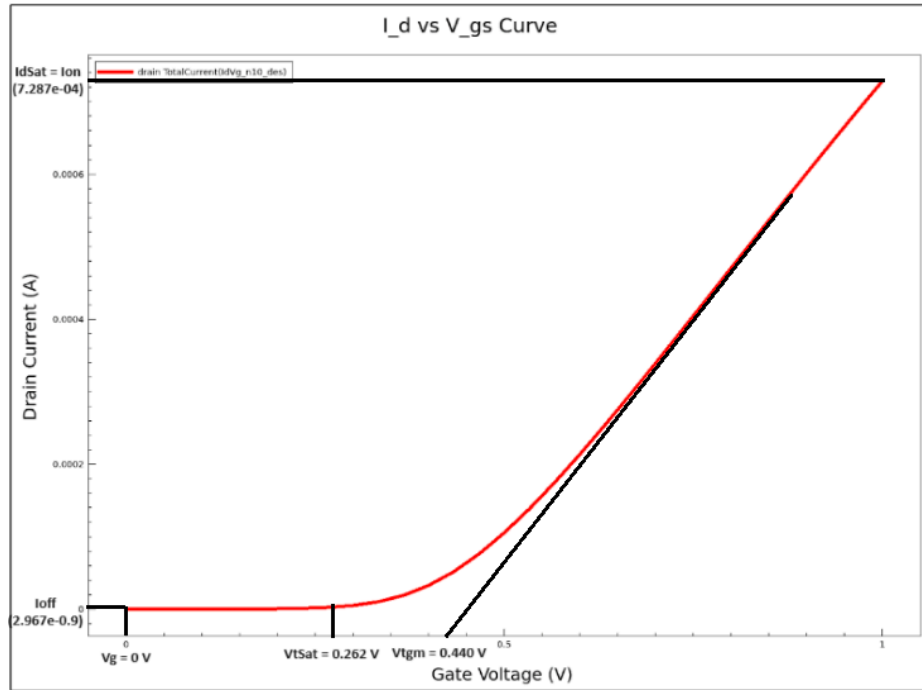


Figure 11:  $I_d$  vs.  $V_{gs}$  curve where  $0 < V_{gs} < V_{dd} = V_{ds} = 1$  V (Saturation)  
 $V_{tSat} = 0.262$  V,  $V_{tgm} = 0.440$  V,  $I_{off} = 2.967 \times 10^{-9}$  A (where  $V_{gs} = 0$  V &  $V_{ds} = V_{dd}$ ) and  
 $I_{on} = I_{dSat} = 7.287 \times 10^{-4}$  A (where  $V_{gs} = V_{ds} = V_{dd} = 1$  V) is marked on the plot.



The threshold voltage in the saturation region ( $V_{tSat} = 0.262$  V) is lower compared to the threshold voltage ( $V_{tLin} = 0.382$  V) in the linear region. This means the transistor enters saturation at a lower  $V_{gs}$ . The drain current is significantly higher at the same  $V_{gs}$  in saturation compared to the linear region, as shown by values of  $I_{dSat}$  and  $I_{dLin}$ .  $I_{off}$ , where the gate voltage is 0, is the same for both regions, whereas  $I_{on}$  is determined by  $I_{dSat}$ . The threshold voltage  $V_{tgm}$  (0.440 V) is at the intersection of the tangent at the maximum  $g_m$  with the  $V_{gs}$  axis.

#### 4. Comparison to TSMC Paper

Based on the results of our final design in *Figure 9*, the subthreshold swing,  $SS_{lin} = 88.525$  mV/decade, and  $SS_{sat} = 87.305$  mV/decade. As stated in the TSMC paper, these values are below 100 mV/decade. Additionally, based on *Figure 9*, our linear threshold voltage,  $V_{tLin} = 0.382$  V, and saturation threshold voltage,  $V_{tSat} = 0.262$  V. In TSMC paper's Figure 4 [6], tracing the 65nm gate length for NFET values we find  $V_{tLin} = 0.2$  V,  $V_{tSat} = 0.15$  V. The trend is of course the same, that is threshold voltage is smaller at saturation than at linear. The values of TSMC are both smaller than ours, this discrepancy may be due to the differences between our ideal simulation setup vs a real physical testing environment of TSMC manufacturing. Physical testing often reveals a lower threshold voltage compared to simulations due to non-idealities and variations that are difficult to capture in simulations.

#### 5. Drain-Induced Barrier Lowering

Drain induced barrier lowering (DIBL) is a short-channel effect in MOSFETs that reduces the threshold voltage of the transistor at higher drain voltages. This effect is negligible in long-channel transistors because the channel formation's 'bottleneck' is sufficiently distant from the drain, ensuring that the drain's electric field does not significantly influence it. In such a scenario, the substrate and gate effectively shield the threshold voltage from any impact of the drain voltage. However, this is no longer true in short-channel devices. The drain is close enough to gate the channel, so a high drain voltage can open the bottleneck and turn on the transistor prematurely [9]. If a high drain voltage is applied, the barrier height can decrease, leading to an increased drain current [10]. We used the equations below to find our design's DIBL [10].

$$DIBL = \frac{\Delta V_{th}}{\Delta V_d} = \frac{|V_{tSat} - V_{tLin}|}{|V_{dsaturation} - V_{dslinear}|} = \frac{|0.262 \text{ V} - 0.382 \text{ V}|}{|1 \text{ V} - 0.05 \text{ V}|} = 126 \text{ mV/V}$$

A smaller DIBL effect implies that the transistor has better control over the premature turn-on process and is less sensitive to changes in the drain voltage.

## 6. Final Design Plot for $I_{ds}$ vs. $V_{ds}$

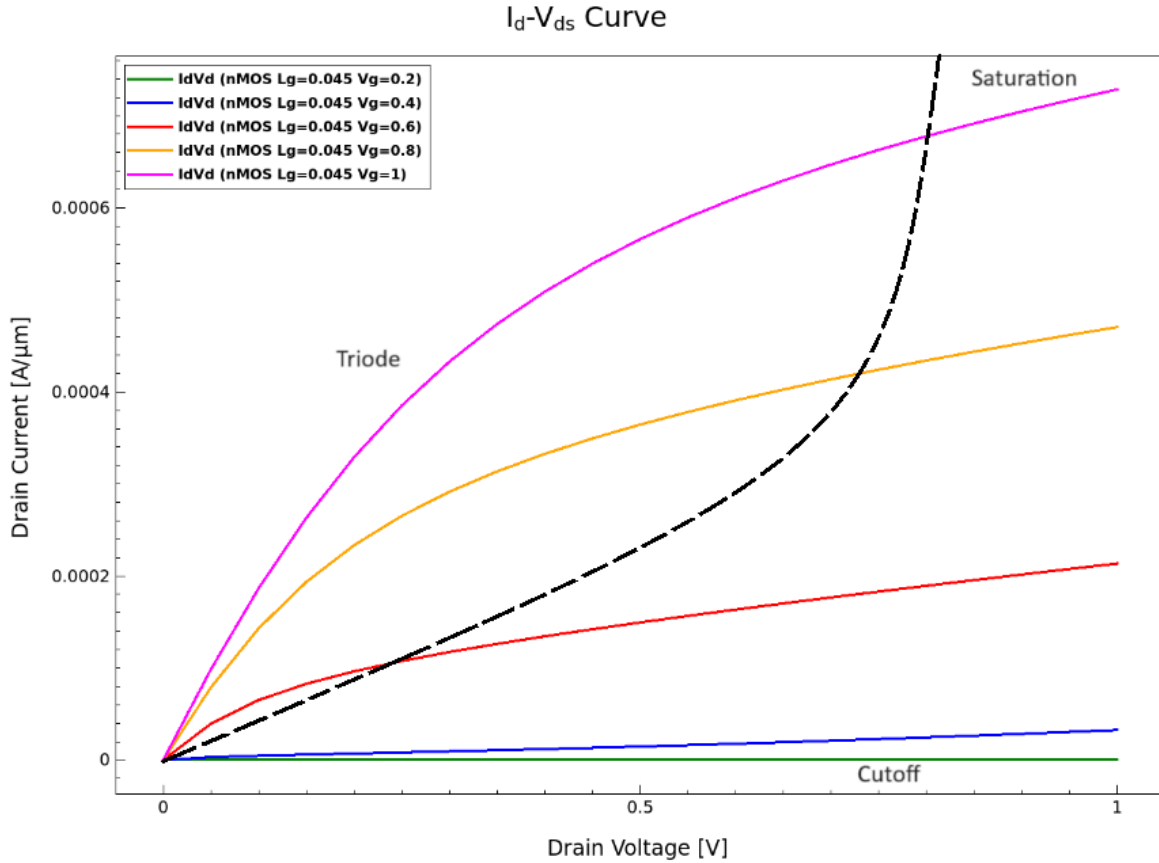


Figure 12:  $I_{ds}$  vs.  $V_{ds}$  curves for  $V_{gs} = 0.2, 0.4, 0.6, 0.8$  and  $1.0$  V for  $0 \leq V_{ds} \leq V_{dd}$ .

The ideal square law dependence for a MOSFET refers to the relationship between the drain current and the gate-to-source voltage in the saturation region. For an ideal MOSFET, where  $I_{ds}$  has no dependency on  $V_{ds}$ , we would expect the curves to be horizontal in the saturation region (see Appendix A). From Figure 12, we observe that the curves are not horizontal as expected, indicating  $I_{ds}$  is dependent on  $V_{ds}$  even in the saturation region. This deviation could be attributed to the short channel effects of the channel length modulation, which causes the drain current  $I_{ds}$  to increase with drain bias  $V_{ds}$  in the saturation region [11].

### C. Bonus

We started with our previous design parameters from Table 1 but with  $V_{dd}=1.2V$ , instead of 1V.

Vtgm	VtiLin	IdLin	SSlin	gmLin	IdSat	Ioff	VtiSat	SSsat	gmSat	Ron
0.440	0.382	1.078e-04	88.564	2.478e-04	1.018e-03	4.590e-09	0.245	87.442	1.364e-03	4205.359

Figure 13: Screenshot of the Sentaurus Workbench with previous design parameters. Although

$$I_{on} = 1018 \mu A/\mu m \geq 445 \mu A/\mu m, \text{ the design specifications are not met as}$$

$$I_{off} = 4.59 nA/\mu m < 0.01 nA/\mu m \text{ for } V_{dd} = 1.2V.$$

As both  $I_{on}$  and  $I_{off}$  are higher than the specification, we first increase the halo doping iteratively to  $6.3 \times 10^{18} \text{ cm}^{-3}$ . Further increasing the halo doping causes an inverse effect, we therefore keep halo at this value and decrease extension doping iteratively to  $3.36 \times 10^{19} \text{ cm}^{-3}$ . At  $3.36 \times 10^{19} \text{ cm}^{-3}$ , neither  $I_{on}$  and  $I_{off}$  met the design specifications, although were close, therefore by keeping extension doping at this value, we increased the substrate doping to  $9.3 \times 10^{17} \text{ cm}^{-3}$ . A list of aforementioned iterations and their results, as well as the final design parameters are presented in Appendix B. Achieved design specifications are presented in Figure 14 below.

Vtgm	VtiLin	IdLin	SSlin	gmLin	IdSat	Ioff	VtiSat	SSsat	gmSat	Ron
0.689	0.651	6.384e-05	91.462	1.756e-04	4.453e-04	9.937e-12	0.569	602.085	9.424e-04	15027.529

Figure 14: Screenshot of the Sentaurus Workbench, showing the achieved device specifications

$$(I_{on} = 445.3 \mu A/\mu m \geq 445 \mu A/\mu m \text{ and } I_{off} = 0.009937 nA/\mu m \leq 0.01 nA/\mu m \text{ for } V_{dd} = 1.2V)$$

### Conclusions

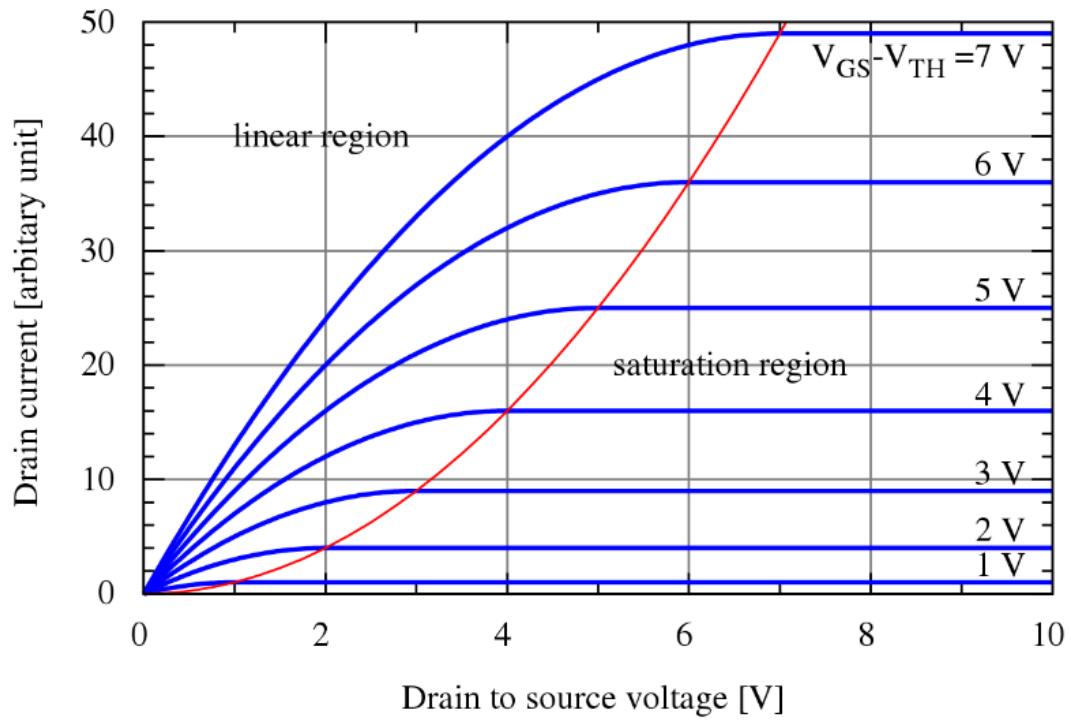
We designed a 45 nm NMOS transistor with a systematic approach observing the effects of reducing or increasing each parameter one at a time. We adjusted physical parameters to meet the desired  $I_{on}$  and  $I_{off}$  criteria and plotted the drain current against the gate-source voltage to observe current trends. Changes in the substrate doping, extension doping and the halo doping concentrations ensured that the final designs met their requirements. We also discussed key terms such as threshold voltages and DIBL along with the readings from TSMC's paper.

## References

- [1] P. Ranade, L. Shifren, and S. R. Sonkusale, "Source/drain extension control for advanced transistors," U.S. Patent US8563384B2, 22 Oct. 2013. [Online]. Available: <https://patents.google.com/patent/US8563384B2/en> (Accessed Dec. 4, 2023)
- [2] A. Erlebach, T. Feudel, A. Schenk, and C. Zechner, "Influence of HALO and drain-extension doping gradients on transistor performance," *Materials Science and Engineering: B*, vol. 114–115, pp. 15-19, 2004. DOI: 10.1016/j.mseb.2004.07.022. [Online] Available: <https://www.sciencedirect.com/science/article/abs/pii/S0921510704003150> (Accessed Dec. 4, 2023)
- [3] R. Wittmann, "1. Introduction," Institute for Microelectronics, TU Wien. [Online]. Available: <https://www.iue.tuwien.ac.at/phd/wittmann/node6.html> (Accessed Dec. 4, 2023)
- [4] M. Rodwell, G. Burek, and L. Weis, "Sidewall Process for III-V MOSFET Fabrication," in 2009 NNIN REU Research Accomplishments, Nanotech at UCSB, Department of Electrical and Computer Engineering, University of California, Santa Barbara, pp. 64-65. [Online] <https://www.nnin.org/sites/default/files/files/2009reura/2009NNINreuWeis.pdf> (Accessed Dec. 4, 2023)
- [5] P. A. Grudowski, "Transistor sidewall spacer stress modulation," U.S. Patent US6902971B2, 7 June 2005. Current Assignee: NXP BV f/k/a Freescale Semiconductor Inc., Shenzhen Xinguodu Tech Co Ltd, NXP BV, North Star Innovations Inc. [Online] <https://patents.google.com/patent/US6902971B2/en> (Accessed Dec. 4, 2023)
- [6] S. K. H. Fung, H. T. Huang, S. M. Cheng, K. L. Cheng, S. W. Waug, Y. P. Wang, Y. Y. Yao, C. M. Chu, S. J. Yang, W. J. Liang, Y. K. Leung, C. C. Wu, C. Y. Lin, S. J. Chang, S. Y. Wu, C. F. Nieh, C. C. Chen, T. L. Lee, Y. Jin, S. C. Chen, L. T. Lin, Y. H. Chiu, H. J. Tao, C. Y. Fu, S. M. Jang, K. F. Yu, C. H. Wang, T. C. Ong, Y. C. See, C. H. Diaz, M. S. Liang, Y. C. Sun, "65nm CMOS High Speed, General Purpose and Low Power Transistor Technology for High Volume Foundry Application," 2004 Symposium on VLSI Technology Digest of Technical Papers, pp. 92-93, 2004.

- [7] "Glossary," INFN Torino Wiki, last updated Sep. 19, 2013. [Online]  
<https://wiki.to.infn.it/vlsi/workbook/glossary> (Accessed Dec. 4, 2023)
- [8] "Sentaurus Technology Template: CMOS Characterization" in TCAD Sentaurus Simulation Project, Synopsys, Inc., 2013.
- [9] "Drain-induced barrier lowering," Wikipedia, last modified Mar. 13, 2023. [Online]  
[https://en.wikipedia.org/wiki/Drain-induced\\_barrier\\_lowering#:~:text=Drain%2Dinduced%20barrier%20lowering%20\(DIBL,transistor%20at%20higher%20drain%20voltages.](https://en.wikipedia.org/wiki/Drain-induced_barrier_lowering#:~:text=Drain%2Dinduced%20barrier%20lowering%20(DIBL,transistor%20at%20higher%20drain%20voltages.) (Accessed Dec. 4, 2023)
- [10] M. Stockinger, "2.3 Drain-Induced Barrier Lowering," Jan. 5, 2000. [Online]. Available:  
<https://www.iue.tuwien.ac.at/phd/stockinger/node15.html> (Accessed Dec. 4, 2023)
- [11] V. Misra and M. C. Öztürk, "3 - Field Effect Transistors," in The Electrical Engineering Handbook, ed. W.-K. Chen, Academic Press, 2005, pp. 109-126. DOI:  
10.1016/B978-012170960-0/50012-8. [Online]. Available:  
<https://www.sciencedirect.com/science/article/pii/B9780121709600500128> (Accessed Dec. 4, 2023)
- [12] "MOSFET," Wikipedia. [Online]. Available: <https://en.wikipedia.org/wiki/MOSFET>  
(Accessed Dec. 4, 2023)

## Appendix A



Appendix A - Figure 1: Example  $I_{ds}$  vs.  $V_{ds}$  curves for an ideal MOSFET, where the curves become horizontal in the saturation region. [12]

## Appendix B

### Iterations of Changed Parameters & Resulting $I_{off}$ and $I_{on}$ Values for the Bonus Part

Appendix B - Table A: Iterations of doping parameters and resulting  $I_{off}$  and  $I_{on}$  values. The parameters that were changed for that iteration are bolded. All other parameters were kept the same as the initial design presented in Table 1 of this report.

Halo Doping [cm <sup>-3</sup> ]	Extension Doping [cm <sup>-3</sup> ]	Substrate Doping [cm <sup>-3</sup> ]	$I_{off}$ [A]	$I_{on}$ [A]
$3.3 \times 10^{18}$	$6 \times 10^{19}$	$9 \times 10^{17}$	$4.59 \times 10^{-9}$	$1.018 \times 10^{-3}$
<b><math>6 \times 10^{18}</math></b>	$6 \times 10^{19}$	$9 \times 10^{17}$	$7.039 \times 10^{-11}$	$5.689 \times 10^{-4}$
<b><math>6.3 \times 10^{18}</math></b>	$6 \times 10^{19}$	$9 \times 10^{17}$	$9.50 \times 10^{-11}$	$5.285 \times 10^{-4}$
$6.3 \times 10^{18}$	<b><math>5 \times 10^{19}</math></b>	$9 \times 10^{17}$	$4.226 \times 10^{-11}$	$5.305 \times 10^{-4}$
$6.3 \times 10^{18}$	<b><math>3 \times 10^{19}</math></b>	$9 \times 10^{17}$	$0.588 \times 10^{-11}$	$4.185 \times 10^{-4}$
$6.3 \times 10^{18}$	<b><math>3.5 \times 10^{19}</math></b>	$9 \times 10^{17}$	$1.184 \times 10^{-11}$	$4.530 \times 10^{-4}$
$6.3 \times 10^{18}$	<b><math>3.3 \times 10^{19}</math></b>	$9 \times 10^{17}$	$0.9114 \times 10^{-11}$	$4.399 \times 10^{-4}$
$6.3 \times 10^{18}$	<b><math>3.4 \times 10^{19}</math></b>	$9 \times 10^{17}$	$1.050 \times 10^{-11}$	$4.466 \times 10^{-4}$
$6.3 \times 10^{18}$	<b><math>3.35 \times 10^{19}</math></b>	$9 \times 10^{17}$	$0.9792 \times 10^{-11}$	$4.432 \times 10^{-4}$
$6.3 \times 10^{18}$	<b><math>3.38 \times 10^{19}</math></b>	$9 \times 10^{17}$	$1.036 \times 10^{-11}$	$4.459 \times 10^{-4}$
$6.3 \times 10^{18}$	<b><math>3.37 \times 10^{19}</math></b>	$9 \times 10^{17}$	$1.007 \times 10^{-11}$	$4.446 \times 10^{-4}$
$6.3 \times 10^{18}$	<b><math>3.36 \times 10^{19}</math></b>	<b><math>9.3 \times 10^{17}</math></b>	$0.9937 \times 10^{-11}$	$4.453 \times 10^{-4}$

Vtgm	VtiLin	IdLin	SSlin	gmLin	IdSat	Ioff	VtiSat	SSsat	gmSat	Ron
0.689	0.649	6.482e-05	91.467	1.777e-04	4.530e-04	1.184e-11	0.566	653.761	9.559e-04	14569.835

*Appendix B - Figure 1: Screenshot of the Sentaurus Workbench, with halo doping set to  $6.3 \times 10^{18} \text{ cm}^{-3}$  and extension doping set to  $3.5 \times 10^{19} \text{ cm}^{-3}$ . (6th iteration)*

Vtgm	VtiLin	IdLin	SSlin	gmLin	IdSat	Ioff	VtiSat	SSsat	gmSat	Ron
0.689	0.649	6.482e-05	91.467	1.777e-04	4.530e-04	1.184e-11	0.566	653.761	9.559e-04	14569.835

*Appendix B - Figure 2: Screenshot of the Sentaurus Workbench, with halo doping set to  $6.3 \times 10^{18} \text{ cm}^{-3}$  and extension doping set to  $3.3 \times 10^{19} \text{ cm}^{-3}$ . (7th iteration)*

Vtgm	VtiLin	IdLin	SSlin	gmLin	IdSat	Ioff	VtiSat	SSsat	gmSat	Ron
0.689	0.650	6.399e-05	91.452	1.760e-04	4.466e-04	1.050e-11	0.568	635.581	9.443e-04	14979.134

*Appendix B - Figure 3: Screenshot of the Sentaurus Workbench, with halo doping set to  $6.3 \times 10^{18} \text{ cm}^{-3}$  and extension doping set to  $3.4 \times 10^{19} \text{ cm}^{-3}$ . (8th iteration)*

Vtgm	VtiLin	IdLin	SSlin	gmLin	IdSat	Ioff	VtiSat	SSsat	gmSat	Ron
0.689	0.650	6.357e-05	91.445	1.752e-04	4.432e-04	9.792e-12	0.569	588.256	9.384e-04	15195.825

*Appendix B - Figure 4: Screenshot of the Sentaurus Workbench, with halo doping set to  $6.3 \times 10^{18} \text{ cm}^{-3}$  and extension doping set to  $3.35 \times 10^{19} \text{ cm}^{-3}$ . (9th iteration)*

#### Appendix B - Changed Final Design Parameters for Bonus Question (sdevice\_des.cmd)

```
; - Substrate doping level
(define SubDop 9.3e17 ) ; [1/cm3]
(define HaloDop 6e18 ) ; [1/cm3]
(define ExtDop 3.36e19) ; [1/cm3]
)
```